JOURNAL OF MATERIALS SCIENCE 17 (1982) 2771–2780

The investigation of metastable ζ-hcp phase in the Ag-rich fcc region of Ag–In alloys rapidly quenched from the melt

V. FRANETOVIĆ, D. KUNSTELJ, A. BONEFAČIĆ
Institute of Physics of the University, Zagreb, P.O. Box 304, 41001 Zagreb, Yugoslavia

Stacking faults, which were detected in the Ag–In system, have been examined by transmission electron microscopy and electron diffraction. An enhanced concentration of stacking faults in splat cooled specimens as well as the formation of a metastable hexagonal phase in the fcc region of the alloy was observed. As far as we know this is the first case of the terminal solid solubility being reduced by rapid quenching. Terminal solid solubility is reduced because of the high concentration of structural defects introduced by quenching, e.g. dislocations and stacking faults, which serve as the nuclei for the transformation from the fcc to the hcp structure. Our measurements and calculations show that the stacking fault energy minimum is shifted to lower electron concentrations with respect to the stacking fault energy minimum corresponding to the equilibrium phase boundary for the fcc–hcp transformation. The new metastable phase boundary for this transformation was confirmed by X-ray examinations. We explain this "earlier" hcp phase appearance in rapid quenched specimens as the consequence of enhanced interaction of the Fermi surface and contracted Brillouin zone. The Brillouin zone contraction we attributed to quenched-in vacancies.

1. Introduction

In recent investigations a number of metastable solid solutions, crystalline and amorphous intermediate phases have been produced by quenching alloys from the liquid state. The majority of these papers deal with the terminal solubility being extended by rapid quenching. For example the shift of the equilibrium phase boundary in the fcc–hcp phase transformation as the result of rapid quenching was considered to be a consequence of the competition between nucleation and growth processes during solidification [1]. In the meantime only a few authors payed attention to the presence of stacking faults (SF) in splat cooled specimens as well as to the variation of stacking fault energy (SFE) with respect to the equilibrium specimens [2, 3].

Here we shall try to explain the experimental data we found in Ag–In alloys rapidly quenched from the melt via stacking fault geometry and energy considerations.

1.1. ζ-phases occurring in the alloys of the noble metals with B sub-group elements

These phases have been included in the group of intermediate phases classified as electron compounds. One of these is the ζ-phase in the Ag–In system investigated here.

A theoretical explanation for the phase boundary position of the primary substitutional solid solution, which is found to be in the region from 1.36 to 1.40 electrons per atom (e_a), and for the formation of hcp phases, was given by the electron theory of Jones [4–6] which was critically reviewed and modified in the works of Massalski

0022–2461/82/102771–10$03.70/0

and King [7–10]. Generally, a fcc structure will change to hcp when the inscribed Fermi sphere (FS) makes contact with the Brillouin zone (BZ) for the fcc lattice (cubic octahedron). If we wish to add more electrons by alloying with a polyvalent component, additional energy is needed once the filled states have reached the zone boundary. The additional electrons can be accommodated only in higher energy states in the next BZ or near the necks of the lower BZ. Thus, it is energetically favourable that the fcc structure changes to one in which the BZ can contain a larger Fermi surface before touching, and that is the hcp structure. Once the hcp structure has formed and more electrons are added by increasing the concentration of polyvalent component, the FS gradually approaches and touches the {1 0 .0} zone faces, which are nearest to the origin in "k"-space [4, 11], causing these faces to move towards the origin. That means the increase of "a"-spacing (Δa) in the hcp phase. A compensating effect is the simultaneous contraction of "c"-spacing, and the result is the fall in the c/a ratio as the electron concentration increases. By measuring "a" and "c" lattice spacings as a function of electron concentration in Ag-based alloys with B sub-group elements it was confirmed [9] that the BZ starts to deform in the narrow region of electron concentration between 1.39 and 1.40 e_a. Namely, all distortion curves (defined as $\Delta a/(a-\Delta a)$ [9] and being the function of e_a) approach to zero at e_a equal to 1.39–1.40 [9]. For the Ag–In system $\Delta a/(a-\Delta a)$ is zero at e_a equal to 1.40 [9], so the ζ-phase can appear when e_a is greater than 1.40. Consequently, the energetical conditions (interaction of the FS and the BZ) for the formation of the equilibrium ζ-phase in the Ag–In system before e_a reaches 1.40 are unfavourable, this phase is most stable when e_a is equal to 1.50 (stable electron compound). It is necessary to emphasize that this theory presumes that both the fcc and hcp phases are not defect structures and that all lattice sites are occupied in each unit cell.

1.2. Stacking faults and stacking fault energy as an indication of the fcc–hcp transformation

Here we would like to emphasize the importance of the introduction of structural defects in the alloy by rapid quenching, particularly stacking faults (SF) and, as far as we can conclude, the essential role of the stacking fault energy (SFE) in the fcc–hcp transformation.

The SF is the defect which makes possible the transformation from one structure to the other, for example from fcc to hcp and vice versa. An intrinsic SF can be formed by motion of a single Shockley partial dislocation in a close packed plane. The motion of such dislocations in every second plane produces bulk hcp crystal. In this way an intrinsic SF can be regarded as the hcp embryo two crystal planes thick. Similarly, an extrinsic fault can be produced by motion of Shockley partials in two consecutive close packed planes. The motion of such dislocations on every close packed plane can produce an fcc twin. In this way the extrinsic fault can be regarded as the fcc twin embryo containing two planes in thickness. Olson and Cohen [12] in their concept of fcc–hcp transformation accepted the following rule: "If the motion of one dislocation per x planes produces a new structure then M such dislocations of proper spacing produce an embryo of that structure with thickness equal to Mx planes". From this point of view bulk phase with hcp (or fcc) structure can be regarded as a pile of neighbouring stacking faults in the fcc (or hcp) matrix. So, if the energetic conditions for heavy faulting are fulfilled, hcp domains could be formed or close packed structures with regular long period stacking sequence could occur in the fcc matrix.

Since we can regard the SFE, γ, in the first approximation as the difference in the free energy between fcc and hcp phase, $\gamma = G^{hcp} - G^{fcc}$ (for the fcc matrix $\gamma > 0$), every increase of free energy of matrix (here G^{fcc}) leads to decrease of SFE. Consequently lower SFE results in an enhanced concentration of stacking faults. By introduction of stacking faults appears the possibility for the formation of the hcp structure in the fcc region of the alloy. Such a hypothesis could be connected with experimentally well established facts [13–15] that the SFE of Ag-based alloys decreases on alloying with a polyvalent component (increasing of e_a) through fcc region and is zero or has a minimal value for e_a which corresponds to the equilibrium phase boundary [14, 15]. (It was predicted by the theoretical models [16–18] that this minimum of SFE exists in noble metal-based alloys and explained as the result of free electron contribution to the SFE.)

If we now pay attention to the behaviour of SFE as a function of temperature, for the elements

or their alloys which crystallize in fcc and/or hcp structures, we encounter similar behaviour [13–15] of the SFE to that of e_a. That is, in the hcp region the SFE decreases when the temperature increases towards the critical value at which transformation occurs and then it increases with temperature in the fcc region. In the works of Ericsson [13] and Gallagher [14] it was shown that SFE is not zero at the temperature of the transformation but has a certain minimal value (see also the model of Hirth [19]).

From the above considerations we can conclude that the SFE is an indication of phase stability. We can expect that the phase transformation fcc $\rightleftarrows$ hcp always occurs for certain e_a, when the narrow region of temperature for which the SFE has a minimal value is encountered. Moreover, we can expect this transformation to occur at some temperature, for a definite e_a for which the SFE is minimal. On this basis various mechanisms [12, 20, 21] of fcc $\rightleftarrows$ hcp transformation via stacking faults were proposed.

1.3. The measurement of stacking fault energy

The determination of SFE by electron microscopy methods is derived from the dislocation interactions. These methods are due to the phenomena which show the existence of planar faults on electron micrographs (nodes, ribbons, multiple ribbons, stacking fault tetrahedra, faulted dislocation dipoles, dislocation loops and twins). For each of those phenomena a set of theory and respective methods [22] exist, by means of which SFE can be estimated. Generally, for each method of direct observation of dislocation configurations it is important to obtain:

(a) random representative sets of defects for measurement, and

(b) a careful insight into the state of material in respect to the local stresses, inhomogeneities of the composition, thermal and mechanical history, etc.

SFE in the Ag–In system is relatively low (from 21 mJ m^{-2} to 5 mJ m^{-2} for e_a from 1.00 to 1.23 [23]). Nevertheless, an estimation of this energy by means of the extended dislocation method [22, 23] can be made. The appropriate equation [22, 23] is:

$$d = \frac{G \cdot b_p^2}{8\pi\gamma} \frac{2-\nu}{1-\nu} \left(1 - \frac{2}{1-\nu} \cos 2\alpha\right) \quad (1)$$

where G and ν are the constants for given material (shear modulus and Poisson ratio respectively), b_p is Burgers vector (BV) modulus of partial dislocation and d is the extension of the node arms at large distances from node (partial dislocations separation). This equation gives the dependence of SFE, γ, as the function of the ribbon width, d, characteristic angle, α (angle between BV and the dislocation), b_p, G, and ν. Detailed solutions of most of the problems which occur in determination of SFE by means of the extended dislocation method can be found in the works of Gallagher [14], Ruff [22], Gallagher and Washburn [23] and Siems [24].

2. Experimental procedure

Seven Ag–In alloys, Ag–11.10, 13.60, 18.40, 22.00, 23.19, 29.15 and 29.70 at% In were prepared from spectroscopically standardized materials. (For details of the preparation see the work of Raynor and Massalski [25].) The chosen region of the Ag–In phase diagram included the α-fcc phase, $\alpha + \zeta$ phase and ζ-hcp phase. After casting, all ingots were homogenized. The alloy compositions are believed to be within ± 0.2 at% on the basis of negligible weight losses during preparation and the reproducibility of the lattice spacing measurements. The concentration homogeneity of ingots was confirmed with the Enraf Guinier–de Wolf focusing camera. The identification of phases was carried out by X-ray and electron diffraction methods.

As we wanted to compare the results of investigations of equilibrium and splat cooled alloys we had to prepare samples for electron microscopy as follows. The as-obtained Ag–In alloys were thinned by the jet-electropolishing method. The electrolyte contained 70 vol% ethanol, 20 vol% $HClO_4$ and 10 vol% glycerine. The thinning was carried out at -20° C (253 K). The same Ag–In alloys were rapidly quenched by our splat cooling apparatus [26]. The temperature of the molten alloys immediately before quenching was maintained at about 100 K above the liquidus. Rapidly quenched foils (splats) were obtained by shock-atomizing of about 50 mg of Ag–In alloy onto a copper substrate held at 90 K. Large areas of flakes were thin enough for transmission electron microscopy without further preparation.

In the electron microscope (EM) investigation we used a Philips EM 300 G electron microscope equipped with a goniometer stage and a rotation holder. To determine the nature of stacking faults

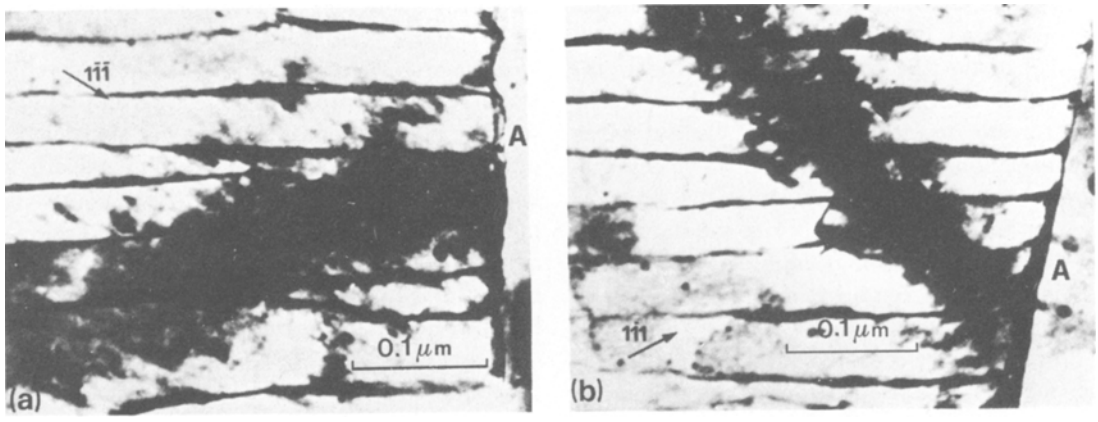

Figure 1 Transmission electron micrographs of an Ag–In alloy rapidly quenched from the melt showing (a) the upper partial dislocations out of contrast, the operating reflection is (1 $\bar{1}$ $\bar{1}$) and A indicates the grain boundary, and (b) the lower partial dislocations out of contrast, the operating reflection is (1 $\bar{1}$ 1) and A again indicates the grain boundary.

we analysed images obtained in the bright and dark fields. This enabled us to distinguish intrinsic and extrinsic stacking faults [27]. The separation of partial dislocations (ribbon width) was measured on enlarged photographs. Corrections for partial dislocation separation were made from the previously determined angle between the fault plane and the crystal orientation. The characteristic angle, α, between **b** and the dislocation line was determined as follows. The sense of $\mathbf{b}_p$ ($b_p^{Ag-In} = 1.67 \times 10^{-10}$ m) could be found with the diffraction vectors $\mathbf{g}_1$ and $\mathbf{g}_2$ for which the partial dislocation is out of contrast. This happens when $\mathbf{b}_p \cdot \mathbf{g}_1 = 0$ and $\mathbf{b}_p \cdot \mathbf{g}_2 = 0$, that is, $\mathbf{b}_p$ is perpendicular to $\mathbf{g}_1$ and $\mathbf{g}_2$. When this procedure is made for both partial dislocations it is possible to determine the characteristic angle, α, from the sense and magnitude of $\mathbf{b}_{p1}$ and $\mathbf{b}_{p2}$. In Fig. 1a and b the upper and lower partial dislocations respectively are invisible. Here the dislocations are parallel with the foil plane (but the fault plane is not). Bend contours due to (1 $\bar{1}$ $\bar{1}$) and (1 $\bar{1}$ 1) diffractions are seen passing across the partials.

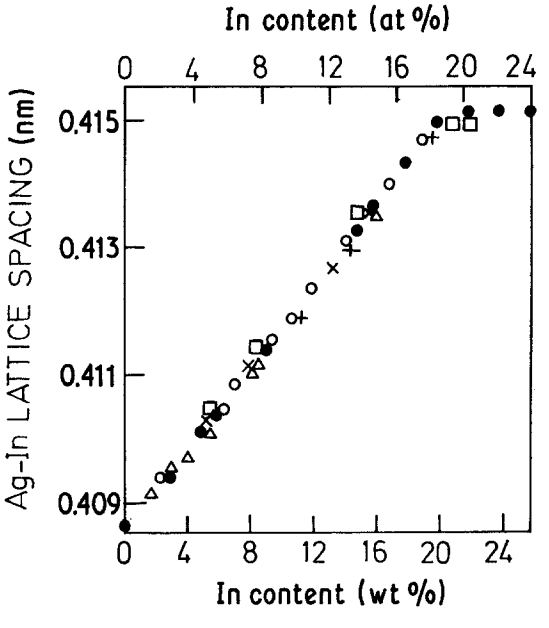

Figure 2 Present lattice spacing measurements of equilibrium Ag–In alloy samples in the fcc region in comparison to the results of other authors, □–Wiebke and Eggers [30], △–Hume-Rothery *et al.* [32], ○–Owen and Roberts [31], X–Adler and Wagner [33], ●–Straumanis and Riad [29] and +–present work.

If all operations have been made with care γ is believed to be within ± 5% [22]. One must bear in mind that the measured SFE is in fact an apparent SFE because of the influence of other defects and surfaces of the specimen. So, it is important to study these ribbons which are as far away from other defects and the specimen surface as possible. This makes additional difficulties in determination of SFE in thin rapidly quenched specimens.

3. Results

3.1. X-ray examinations

An analysis of X-ray diffraction lines was made to compare equilibrium and splat cooled samples. A very good agreement with the equilibrium phase diagram [28] and the measurements of other authors [29–31] was achieved in the fcc region (Fig. 2). In this figure the results for rapidly quenched specimens a_{rq} of Ag–13.60 at% In (e_a = 1.27) and Ag–18.40 at% In (e_a = 1.37) are not marked but we report them explicitly: a_{rq} (e_a =

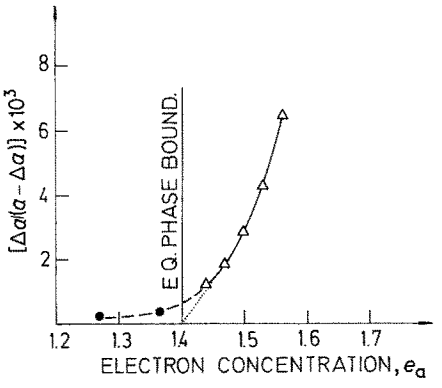

Figure 3 Plot of distortion parameter, $\Delta a/(a-\Delta a)$, against electron concentration (e_a) showing results for equilibrium samples (△), King and Massalski [9] and rapidly quenched samples (•), present work.

1.27) = 0.41300 nm and a_{rq} ($e_a = 1.37$) = 0.41460 nm. Corresponding equilibrium values, which may be found in Fig. 2, are: a_{eq} ($e_a = 1.27$) = 0.41290 nm and a_{eq} ($e_a = 1.37$) = 0.41445 nm. This shows that the lattice parameters in rapidly quenched specimens are somewhat greater than the equilibrium values, and the distortion parameter [9], $\Delta a/(a-\Delta a)$, can be calculated: For $e_a = 1.27$ $\Delta a/(a-\Delta a) = 0.24 \times 10^{-3}$ and for $e_a = 1.37$ $\Delta a/(a-\Delta a) = 0.36 \times 10^{-3}$ (Fig. 3). As a consequence of the lattice distortions (Fig. 3) the hexagonal stacking of atoms is favoured. (Positive Δa means the contraction of the BZ and, from the standpoint of the BZ–FS interaction, this is equivalent to an e_a increase.) So, by rapid quenching of Ag–18.40 at% In, which is in equilibrium with pure f c c phase, we obtained X-ray patterns on which diffraction lines of the h c p phase were also present. Quenched samples were then submitted to thermal treatment in evacuated tubes of fused quartz. X-ray patterns of annealed samples showed no diffraction lines of the h c p phase. The existence of the metastable h c p phase in the Ag–18.40 at% In alloy, here obtained by rapid quenching, was so confirmed.

Furthermore, by rapid quenching of the Ag–22.00 at% In alloy (two-phase region) we obtained the X-ray patterns which showed the reversal of intensities of diffraction lines belonging to the f c c and h c p phases in respect of the line intensities of equilibrium samples. That is, the relative amount of h c p phase present in splat cooled samples was enhanced with respect to the f c c phase. The increase of the amount of h c p phase present in splat cooled samples was about 50% in relation to its equilibrium content. After annealing, X-ray diffraction patterns were the same as the one obtained from the equilibrium samples, the surplus of the h c p phase transformed to the f c c structure.

A similar effect was also obtained by rapid quenching of the Ag–23.20 at% In alloy (two-phase region). All these results show that h c p stacking is preferred to the f c c stacking sequence in splat cooled samples in comparison with the equilibrium. It means that the shift of the f c c–h c p phase boundary towards smaller e_a values was caused by rapid quenching. That is, a new metastable hexagonal phase in the Ag–In system was obtained by rapid quenching from the melt, with lower electron concentration than the equilibrium ζ-phase.

For a comparison with non-equilibrium samples, the control group of equilibrium Ag–In alloys was investigated. In our measurements of the position of the equilibrium boundary for the solid solubility of indium in silver an agreement was obtained with the work of Straumanis and Riad [29] who found that the equilibrium solubility is 20.4 wt% In in contrast to the previous 19.2 wt% In [30]. We also identified diffraction lines on X-ray patterns of equilibrium Ag–29.15 at% In and Ag–29.70 at% In and confirmed that these alloys are of the close packed hexagonal structure, that is the ζ (Ag_3In) phase of Cd_3Mg type, the same as stated in the work of Uemura and Satow [34]. The ζ-phase with 25 at% In, above 300° C, has lattice spacings of $a = 0.2954$ nm and $c = 0.4804$ nm, so the ratio $c/a = 1.626$ [28], and transforms at 214° C to the ζ′ ordered structure [34]. We checked this order–disorder transformation by the technique of differential thermal analysis and obtained the second order phase transformation at 200° C without a change of crystal structure (i.e. the same c/a). In two-phase equilibrium alloys, Ag– 22.00 at% In and Ag–23.19 at% In, the relative amounts of phases present were in good agreement with those of Massalski and King [9].

3.2. EM examinations

Here we report an EM study of the stacking faults in Ag–In alloys rapidly quenched from the melt and the measurement of the stacking fault energy using the technique of direct observation of dislocation configurations.

Our examinations of structure defects by TEM have shown that in splat cooled specimens of Ag–In almost all phenomena connected to stacking

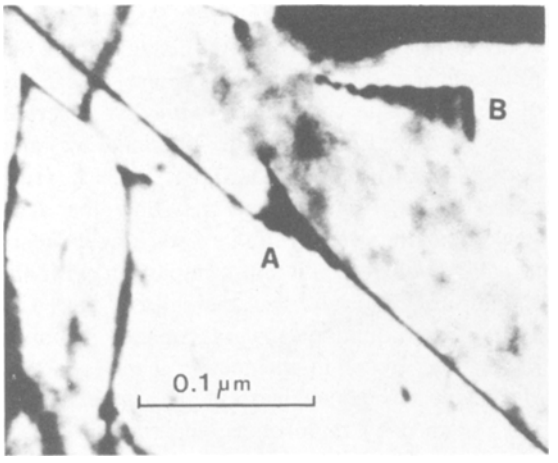

Figure 4 Transmission electron micrograph of the Ag–18.4 at% In alloy rapidly quenched from the melt showing A the dislocation node and B the partially developed stacking fault.

faults can be found: we observed ribbons, double ribbons, twins but rarely nodes. The nodes were in the most cases very distorted and thus unfavourable for SFE measurements. On a typical transmission electron micrograph (Fig. 4) of Ag–18.40 at% In one isolated extended dislocation node (A) and the stacking fault (B) can be seen. In rapidly quenched specimens of the Ag–18.40 at% In alloy a lamellar structure was also frequently detected (Fig. 5). The width of these twin lamellae is on average about a few tens of nanometers. The EM examinations showed that the concentration of SF in splat cooled specimens (Fig. 6a) is much greater than in the same alloy in equilibrium (Fig. 6b), and it is greatest in the vicinity of the f c c–h c p phase boundary.

Measurements and calculation of SFE were performed using the EM methods and the equation briefly discussed in the Introduction. The ribbon method we applied provides, at present, the most accurate results in the low SFE range. Material constants G and ν for a given e_a were taken from recent works [23, 35]. We paid special attention to the quenched alloys near the phase boundary, so the SFE was measured for e_a equal to 1.22, 1.27, 1.37 and 1.44. We found that the characteristic angle, α, was close to 30° in all alloys, which seems to be the most usual value [36, 37]. The average values of the SFE ($\bar{\gamma}$), calculated from ribbon widths for four different e_a are presented in Table I and Fig. 7. The uncertainty, $\Delta\gamma$, caused by uncertainties in the measurement of ribbon widths, was up to 0.3 mJ m^{-2}. In Fig. 7 the metastable boundary is marked with respect to the equilibrium. It can be seen that the minimum value of SFE in the splat cooled specimens determines the new (metastable) phase boundary, just as the minimum of SFE in the equilibrium samples always corresponds to the equilibrium phase boundary.

4. Discussion and conclusions

It is not possible to explain the appearance of the ζ-hexagonal metastable phase at e_a less than 1.4 assuming the equilibrium theory of Jones and Massalski [4–11]. However, if we keep in mind that the theory proposes the f c c and h c p phases as being structures without defects, we are looking for the reasons for formation of hexagonal domains

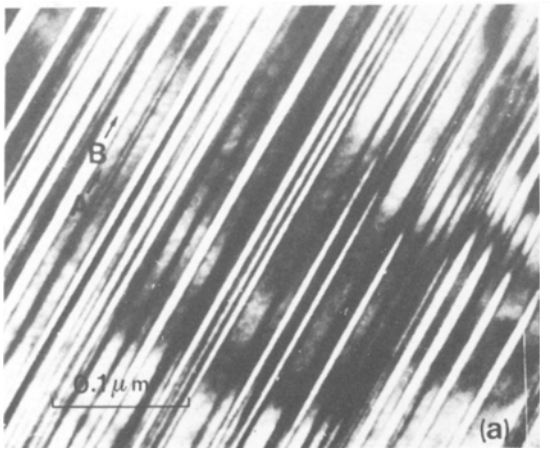

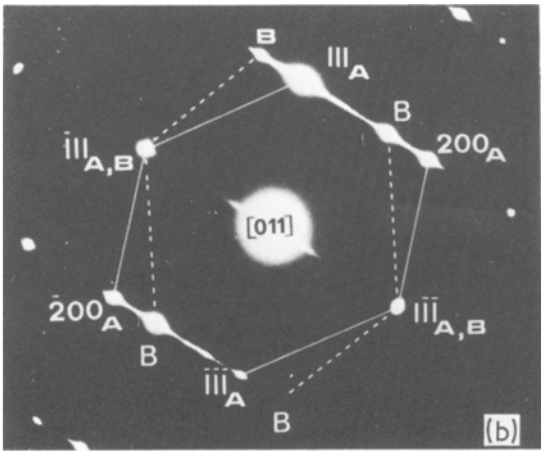

Figure 5 Ag–18.4 at% In alloy rapidly quenched from the melt showing (a) narrow twin lamellas and (b) the corresponding diffraction pattern. Crystallographic relations of the twin lamellas A and B were determined by the diffraction pattern, as indicated in (a) and (b).

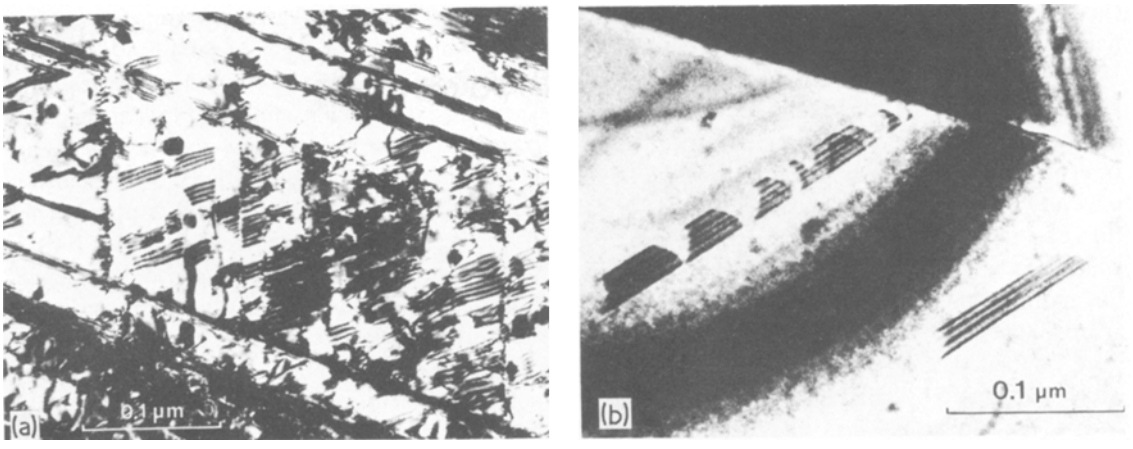

Figure 6 Stacking faults in (a) rapidly quenched Ag–13.6 at% In alloy and (b) equilibrium Ag–13.6 at% in alloy.

in the f c c region in changed energetical conditions introduced by rapid quenching.

For this purpose we suggest that the transformation from f c c to h c p structure takes place via a stacking fault mechanism for the following reasons:

(a) An enhanced concentration of SF in all splat cooled specimens was achieved by rapid quenching (frozen-in defects, Fig. 6a).

(b) It was found that the SFE in splat cooled specimens is lower than in equilibrium (Table I, Fig. 7).

(c) By measuring the SFE in splat cooled specimens the minimum value was obtained for lower e_a than found by other authors (Fig. 7). This minimum corresponds to the new (metastable) phase boundary (Fig. 7), which was confirmed by our X-ray measurements.

(d) A positive change, Δa, of the lattice spacing (Fig. 3) means contraction of the Brillouin zone and, consequently, earlier overlap of the Fermi surface. This promotes h c p stacking.

Previous experimental and theoretical results have shown that the minimum of SFE corresponds to that e_a at which the transformation from f c c to h c p occurs (Fig. 3). Now, the new minimum determines the metastable phase boundary in splat cooled specimens (Fig. 7). The geometrical conditions for this transformation are fulfilled in our system (Figs 1, 5 and 6), as well as the energetical conditions (low SFE, Fig. 7). All this is the effect of rapid quenching, as confirmed by the disappearance of the metastable hexagonal phase upon annealing.

TABLE I

e_a	Number of measurements	Number of specimens	$\bar{\gamma}$ (mJ m^{-2})	$\pm \Delta\gamma$ (mJ m^{-2})
1.22	75	5	4.95	0.25
1.27	60	5	4.80	0.22
1.37	39	5	3.70	0.10
1.44	43	5	6.23	0.23

On the basis of our results we do not insist here on the specific kind of transformation from f c c to h c p via stacking faults, but let us mention that it has already been shown for rapidly quenched Ag–Ge alloy [38] that the h c p phase was formed as a result of profuse faulting of the highly supersaturated f c c solid solution of Ge in Ag. It was also suggested [38] that the reverse transformation, that is, the h c p decomposition, is also induced by incidence and growth of f c c stacking faults within the crystals of the metastable h c p phase. Furrer *et al.* [3] proposed that the metastable hexagonal phase achieved by rapid quenching of the Ag–Ge system was formed via stacking faults,

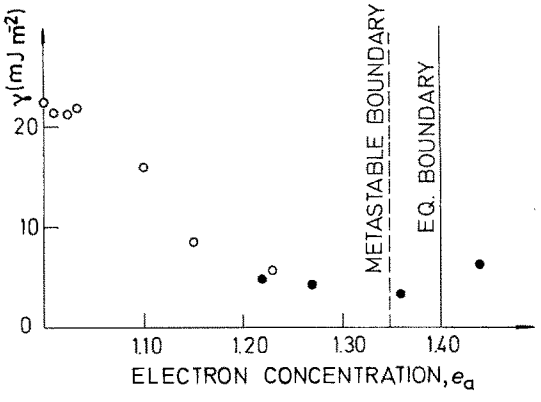

Figure 7 Results of SFE measurements on equilibrium samples of Ag–In alloys (Gallagher [14], for e_a up to 1.23) and splat cooled samples (present work, for e_a near the f c c–h c p transition).

(his conclusions were based only on EM examinations, and no SFE measurements).

These considerations could be understood if we keep in mind that stacking faults could be regarded as embryos of the new phase and the macrostructure of that phase as a stacking of intrinsic faults on every second plane. It means that the formation of a regular close packed structure (e.g. h c p), which present regularly piled-up stacking faults in the matrix of the other close packed structure (e.g. f c c) is possible. Similar long period structures were obtained by martensitic transformation which was caused by rapid quenching [3].

Let us emphasize that the effect of rapid quenching in our case was the same as alloying with polyvalent components (i.e. an increase of e_a). The decrease of SFE and consequent enhancement of SF concentration caused an unstable relation between the stacking faults and the matrix for a given e_a, and the formation of hexagonal domains was thus possible.

The lattice spacing measurements and the plot of the distortion curve $\Delta a/(a-\Delta a)$ as a function of e_a (Fig. 3) show that "a"-spacing is expanded in the rapidly quenched samples. This would imply that a certain amount of distortion had remained after quenching, so the disappearance of the $\Delta a/(a-\Delta a)$ curve is moved towards lower e_a (Fig. 3). For this reason there is a possibility for formation of ζ-phase at e_a equal to 1.37, that is, less than 1.40 e_a, the equilibrium ζ-phase boundary.

To clarify the above statements we must recall that an excess of vacancies is introduced by rapid quenching from the melt, as well as a high concentration of dislocations, stacking faults and twins. Some vacancies condense to form dislocation loops (with h c p stacking of atoms) and serve as the embryos for the formation of stacking faults as well as the extended dislocation does. The driving force for SF growth, the formation of the long period SF sequences and consequently the h c p ζ-phase appearance, is generated by the distortion $\Delta a/(a-\Delta a)$. Positive change of the lattice parameter (Fig. 3), i.e. a contraction of the Brillouin zone, is due to quenched-in vacancies. This change can be estimated as follows. Deplanté and Blandin [39] have calculated changes of the lattice parameter induced by foreign atoms of valency different to that of matrix. So, if we assume a vacancy as being an "impurity" of zero charge, we can estimate the lattice parameter change of pure Ag and Ag–In alloys due to quenched-in vacancies. The results of the calculations are $(\Delta a/ac_v)_{Ag} = 0.023$ and $(\Delta a/ac_v)_{Ag-In} = 0.043$, 0.041 and 0.040 for $e_a = 1.27$, 1.37 and 1.40 respectively, where c_v is the concentration of quenched-in vacancies. These results show that (a) the change of the lattice parameter, due to quenched-in vacancies, of Ag and Ag–In alloys is positive, and (b) the e_a ratio, ranging from 1.27 to 1.40 in present calculations, poorly influences this change. (Since c_v is unknown, we cannot compare quantitatively the results obtained by FDB calculations [39] to the experimental data in Fig. 3.)

We see that there are two processes in parallel, extension of the Fermi surface due to alloying of monovalent Ag with trivalent In and the contraction of the Brillouin zone due to quenched-in vacancies. Both of these events promote the f c c to h c p transformation in quenched Ag–In alloys by lowering the free electron energy via Fermi surface–Brillouin zone interaction. This happens at lower e_a than the equilibrium 1.4 value, that is an "earlier" overlap of the Brillouin zone by the Fermi surface occurs in the metastable rapidly quenched Ag–In alloys.

Acknowledgements

The authors are grateful to D. Subašić for the DTA measurements, to V. Lepčin for technical assistance and to J. Cooper for reading and commenting on the manuscript.

Appendix: $(\Delta a/ac_v)_{Ag-In}$ calculations using the oscillating potential method [39–41]

$$\left(\frac{\Delta a}{ac}\right) = \frac{\chi n Z e^2}{18\Omega\pi k_F} \cdot \frac{\alpha \sin(2k_F r_0' + \phi)}{r_0'^2} \text{(in e.s.u.)}$$

where $(\Delta a/ac)$ is the relative change of the lattice parameter due to the quenched-in impurities of concentration c; χ is the compressibility of the matrix; n the number of closest neighbours; Z the valency of the matrix; e the charge of the electron; Ω the crystal volume per atom; k_F the Fermi electron wave vector; r_0' the distance host atom–impurity; α and ϕ are given by [39]:

$$\alpha \sin\phi = 2\sum_l (-1)^l (2l+1) \sin^2\eta_l(k_F)$$

$$\alpha \cos\phi = 2\sum_l (-1)^l (2l+1) \sin\eta_l(k_F) \times \cos\eta_l(k_F)$$

where $\eta_l(k_F)$, the phase shifts of the lth symmetry, are determined by the Friedel's sum rule [42]:

$$\frac{2}{\pi}\sum_l (2l+1)\eta_l = \Delta Z \equiv Z' - Z$$

(Z' is the valency of the impurity), relating the differences in charge between host atom and impurity to the phase shifts η_l of the conducting electrons, produced by the perturbing potential at the Fermi level. This rule ensures a complete screening of the impurity at large distances and so it preserves the neutrality of a sample.

Now we calculate the lattice parameter change of pure Ag and some Ag–In alloys due to the quenched-in vacancies.

(1) Pure silver: $Z = Z_{Ag} = 1$, $Z' = Z_V = 0$, that is, we take the vacancy as the "impurity" of zero charge, so $\Delta Z \equiv Z_V - Z_{Ag} = -1$. We take $l = 0$, that is, only s-electrons from the top of the Fermi distribution are supposed to be captured by the perturbing potential at the place of vacancy, making a virtually bound state [39]:

$$\frac{2}{\pi}\sum_l (2l+1)\eta_l(k_F) = \frac{2}{\pi}\eta_0(k_F) = -1,$$

so;

$$\eta_0 = -\frac{\pi}{2}.$$

The wave-number, k_F, we calculate in the "free electron approximation" [43]:

$$E_F = 36.1\left(\frac{n_0}{\Omega_0}\right)^{2/3}(\text{eV}) \quad n_0 = \frac{e}{a} = Z_{Ag} = 1$$

$$\Omega_0 = \frac{(a_0^{Ag})^3}{4},$$

$$a_0^{Ag} = 0.4086\,\text{nm} = 4.086 \times 10^{-8}\,\text{cm},$$

so

$$\Omega_0 = 0.0171\,\text{nm}^3 = 17.1 \times 10^{-24}\,\text{cm}^3$$

and

$$E_F^{Ag} = 36.1\,(1/17.1)^{2/3} = 5.44\,\text{eV}$$

([43], p. 54: $E_F^{Ag} = 5.52\,\text{eV}$). Now

$$k_F^{Ag} = \frac{2\pi}{h}\sqrt{(m_e E_F^{Ag})}$$

and $h = 6.63 \times 10^{-34}$ J sec, $m_e = 9.11 \times 10^{-31}$ kg, $E_F^{Ag} = 5.44\,\text{eV} = 8.7584 \times 10^{-19}$ J, so $k_F^{Ag} = 1.2 \times 10^{10}\,\text{m}^{-1} = 1.2 \times 10^8\,\text{cm}^{-1}$.

$r_0' \cong 2r_0^{Ag} = 2a_0^{Ag}\sqrt{2}/4 = 2.89 \times 10^{-8}$ cm is the approximate distance host atom–vacancy.

$$2k_F r_0' = 6.924\,\text{rad} \quad \sin 2k_F r_0' = 0.5979$$

$$\cos 2k_F r_0' = 0.8016$$

$l = 0$ (s-electrons), $\alpha \sin\phi = 2\sin^2\eta_0 = 1$

$$\alpha \cos\phi = 2 \sin\eta_0 \cos\eta_0 = 0$$

$$\chi_{Ag} \cong 10^{-12}\,\text{cm}^2\,\text{din}^{-1},\ n = 12,\ Z \equiv Z_{Ag} = 1,$$

$$e = 4.83 \times 10^{-10}\,\text{e.s.u.}\ (1.61 \times 10^{-19}\,\text{C})$$

$$\frac{\chi_{Ag} \cdot n \cdot Z_{Ag} \cdot e^2}{18\Omega_0 \pi k_F^{Ag} \cdot r_0'^2} \equiv A_1 = 0.03,$$

and

$$\left(\frac{\Delta a}{a c_v}\right)_{Ag} = A_1(\alpha \cos\phi \cdot \sin 2k_F^{Ag} r_0' + \alpha \sin\phi \cdot \cos 2k_F^{Ag} r_0') = 0.023.$$

That is $(\Delta a/ac_v)_{Ag} = 0.023 > 0$, i.e. lattice expansion due to quenched-in vacancies.

(2) Ag–1.27(e_a)In, $Z = 1.27$, $Z' \equiv Z_V = 0$, $Z = -1.27$, $\eta_0 = -0.635\pi = -114.3°$

$$\alpha \sin\phi = 2\sin^2\eta_0 = 1.6613$$

$$\alpha \cos\phi = 2 \sin\eta_0 \cdot \cos\eta_0 = 0.7501$$

$$E_F = 36.1\,(1.27/17.1)^{2/3} = 6.38\,\text{eV}$$

$$k_F = 1.2 \times 10^8\,\text{cm}^{-1} \quad 2k_F r_0' = 7.514\,\text{rad}$$

$$A_{1.27} = 0.034 \text{ and } (\Delta a/ac_v)_{1.27} = 0.043 > 0.$$

(3) Ag–1.37(e_a)In, $Z = 1.37$, $Z' \equiv Z_V = 0$, $Z = -1.37$, $\eta_0 = -1.37 \times \pi/2 = -123.3°$

$$\alpha \sin\phi = 2\sin^2\eta_0 = 1.3971$$

$$\alpha \cos\phi = 2 \sin\eta_0 \cos\eta_0 = 0.9178$$

$$E_F = 36.1\,(1.37/17.1)^{2/3} = 6.71\,\text{eV},$$

$$k_F = 1.33 \times 10^8\,\text{cm}^{-1}$$

$$2k_F r_0' = 7.685\,\text{rad}, \quad \sin 2k_F r_0' = 0.9858$$

$$\cos 2k_F r_0' = 0.1682$$

$$A_{1.37} = 0.036 \text{ and } (\Delta a/ac_v)_{1.37} = 0.041 > 0$$

(4) Ag–1.4(e_a)In, $Z = 1.4$, $Z' \equiv Z_V = 0$; $Z = -1.4$, $\eta_0 = -1.4\pi/2 = -126°$

$$\alpha \sin\phi = 2\sin^2\eta_0 = 1.309$$

$$\alpha \cos\phi = 2 \sin\eta_0 \cos\eta_0 = 0.9511$$

$$E_F = 36.1\,(1.4/17.1)^{2/3} = 6.8\,\text{eV},$$

$$k_F = 1.34 \times 10^8\,\text{cm}^{-1}$$

$$2k_F r_0' = 7.7363\,\text{rad} \quad \sin 2k_F r_0' = 0.9931$$

$$\cos 2k_F r_0' = 0.1174$$

$$A_{1.4} = 0.036 \text{ and } (\Delta a/ac_v)_{1.4} = 0.04 > 0.$$

Acknowledgement

This work was supported through the funds made available to the US–Yugoslav Joint board on Scientific and Technological Co-operation.

References

1. W. KLEMENT, Jr, *Trans. Met. Soc. AIME* **223** (1965) 1182.
2. P. RAMACHANDRARAO and T. R. ANANTHARAMAN, *Phil. Mag.* **20** (1969) 201.
3. P. FURRER, T. R. ANANTHARAMAN and H. WARLIMONT, *ibid.* **21** (1970) 873.
4. N. F. MOTT and H. JONES, "The Theory of the Properties of Metals and Alloys" (Dover Publishers, New York, 1958).
5. H. JONES, *Proc. Roy. Soc. A* **144** (1934) 225.
6. *Idem, Proc. Phys. Soc.* **49** (1937) 243.
7. T. B. MASSALSKI and H. W. KING, *Acta Met.* **10** (1962) 1171.
8. T. B. MASSALSKI, *ibid.* **5** (1957) 541.
9. H. W. KING and T. B. MASSALSKI, *Phil. Mag.* **6** (1961) 669.
10. T. B. MASSALSKI, *J. Phys. Rad.* **23** (1962) 647.
11. H. JONES, *Proc. Roy. Soc. A* **147** (1934) 396.
12. G. B. OLSON and M. COHEN, *Met. Trans.* **7A** (1976) 1897.
13. T. ERICSSON, *Acta Met.* **14** (1966) 853.
14. P. C. J. GALLAGHER, *Met. Trans.* **1** (1970) 2429.
15. A. W. RUFF and L. K. IVES, *Phys. Stat. Sol. (a)* **16** (1973) 133.
16. A. BLANDIN, J. FRIEDEL and G. SAADA, *J. Phys.* **27** (1966) C3–128.
17. T. C. TISONE, R. C. SUNDAHL and G. Y. CHIN, *Met. Trans.* **1** (1970) 1561.
18. T. C. TISONE, *Met. Trans.* **3** (1972) 427.
19. J. P. HIRTH, *ibid.* **1** (1970) 2367.
20. W. BOLLMANN, "Crystal Defects and Crystalline Interfaces" (Springer-Verlag, Berlin, 1970).
21. J. W. CRISTIAN and P. R. SWAN, in "Alloying Behaviour and Effects in Concentrated Solid Solutions", edited by T. B. Massalski (Gordon and Breach, New York, 1965).
22. A. W. RUFF, Jr, *Met. Trans.* **1** (1970) 2391.
23. P. C. J. GALLAGHER and J. WASHBURN, *Phil. Mag.* **14** (1966) 971.
24. R. SIEMS, *Disc. Faraday Soc.* **38** (1964) 42.
25. G. V. RAYNOR and T. B. MASSALSKI, *Acta Met.* **3** (1955) 480.
26. V. FRANETOVIĆ, O. MILAT, D. IVČEK and A. BONEFAČIĆ, *J. Mater. Sci.* **14** (1979) 498.
27. S. AMELINCKX, "The Direct Observation of Lattice Defects by means of Electron Microscopy", paper presented at the 8th Yugoslav Summer School of Physics, Hercegnovi, 1963.
28. M. HANSEN, "Constitution of Binary Alloys" (McGraw-Hill Book Co., London, 1958).
29. M. E. STRAUMANIS and S. D. RIAD, *Trans. Met. Soc. AIME* **233** (1965) 964.
30. F. WEIBKE and H. EGGERS, *Z. Anorg. Allgem. Chem.* **222** (1935) 145.
31. E. A. OWEN and E. W. ROBERTS, *Phil. Mag.* **27** (1939) 294.
32. W. HUME-ROTHERY, G. F. LEWIN and P. W. REYNOLDS, *Proc. Roy. Soc. A* **157** (1936) 167.
33. R. P. I. ADLER and C. N. J. WAGNER, *J. Appl. Phys.* **33** (1962) 3451.
34. O. UEMURA and T. SATOW, *Trans. Japan Inst. Met.* **14** (1973) 199.
35. R. BACON and C. S. SMITH, *Acta Met.* **4** (1956) 337.
36. P. B. HIRSCH, A. HOWIE and M. J. WHELAN, *Phil. Trans. Roy. Soc. A* **252** (1960) 499.
37. A. W. RUFF and L. K. IVES, *Acta Met.* **15** (1967) 189.
38. H. O. K. KIRCHNER, P. RAMANCHANDRARAO and G. A. CHADWICK, *Phil. Mag.* **25** (1972) 1151.
39. J. L. DEPLANTÉ and A. BLANDIN, *J. Phys. Chem. Solids* **26** (1965) 381.
40. A. BLANDIN and L. J. DEPLANTÉ, *J. Phys. Rad.* **23** (1962) 609.
41. A. BLANDIN, in "Alloying Behaviour and Effects in Concentrated Solid Solutions", edited by T. B. Massalski (Gordon and Breach, New York, 1965) p. 50.
42. J. FRIEDEL, *Adv. Phys.* **3** (1954) 446.
43. N. F. MOTT and H. JONES, "The Theory of the Properties of Metals and Alloys" (Dover, New York, 1958) p. 54.

Received 21 September
and accepted 14 December 1981